Case Studies in Thermal Engineering 59 (2024) 104541

Contents lists available at ScienceDirect

Case Studies in Thermal Engineering

journal homepage: www.elsevier.com/locate/csite

Novel exterior insulation finishing: Enhancing building energy efficiency and flame-retardancy through thermal storage and fire propagation prevention

Seunghwan Wi [a], Young Uk Kim [b], Seong Jin Chang [c], Umberto Berardi [d], Sumin Kim [b,*]

[a] *School of Architecture, Seoul National University of Science and Technology, Seoul 01811, Republic of Korea*
[b] *Department of Architecture and Architectural Engineering, Yonsei University, Seoul 03722, Republic of Korea*
[c] *College of Construction and Environmental Engineering, Gyeongsang National University, Jinju, 52725, Republic of Korea*
[d] *Canada Research Chair in Building Science, Department of Architectural Science, Toronto Metropolitan University, Toronto, ON, M5B 2K3, Canada*

A R T I C L E I N F O

Keywords:
Exterior insulation finishing
Fire spread prevention
Thermal insulation
Thermal storage
Heat transfer
Energy efficiency

A B S T R A C T

Exterior insulation finishing systems (EIFSs) can efficiently promote energy efficiency of buildings. In this study, an EIFS with high thermal efficiency is presented to improve the insulation behavior of building enclosure. Based on heat transfer analysis results, energy simulations of buildings with fire spread prevention structures were performed. Results revealed that heat flow through the wall increased by 10.3 % when using a metal rail to fix the insulation; in contrast, using non-combustible phenolic foam reduces heat flow by 37.4 %, satisfying the requirement for fire spread prevention structures. Additionally, the energy consumption decreased by 8.8 % when both mineral wool and phenolic foam were applied. Fire spread prevention structures are essential to improve the fire safety performance of buildings. This external insulation system efficiently promote energy saving in building; additionally, leveraging a phase change material to improve the thermal storage performance of the building can reduce energy consumption by up to 11.9 %.

1. Introduction

Global energy consumption has increased owing to the rapid population growth and urbanization following industrialization; in particular, the energy consumption of buildings currently accounts for 40 % of the total energy consumption worldwide [1,2]. Therefore, following the Paris Agreement, policies to reduce greenhouse gas emissions by 2030 and achieve carbon neutrality by 2050 were proposed worldwide [3]. The most effective approach to reducing the energy consumption of buildings entails improving their insulation effect. Thus, the development of aerogel [4–7] vacuum [8–10], and super-resistant insulation materials [11–13] has been actively emphasized. In the interior thermal insulation construction method, thermal bridges occur in areas in contact with the structures [14,15]; these thermal bridges can be prevented by reinforcing the insulation of the joints and thermal cross-blocking [16]. However, the external insulation method is more effective in terms of preventing unnecessary thermal energy losses because it does not cause thermal bridges [17]. Notably, the exterior insulation plastering finishing method, introduced in the 1950s, involves applying a

* Corresponding author.
E-mail address: kimsumin@yonsei.ac.kr (S. Kim).

https://doi.org/10.1016/j.csite.2024.104541
Received 25 February 2024; Received in revised form 23 April 2024; Accepted 11 May 2024
Available online 14 May 2024

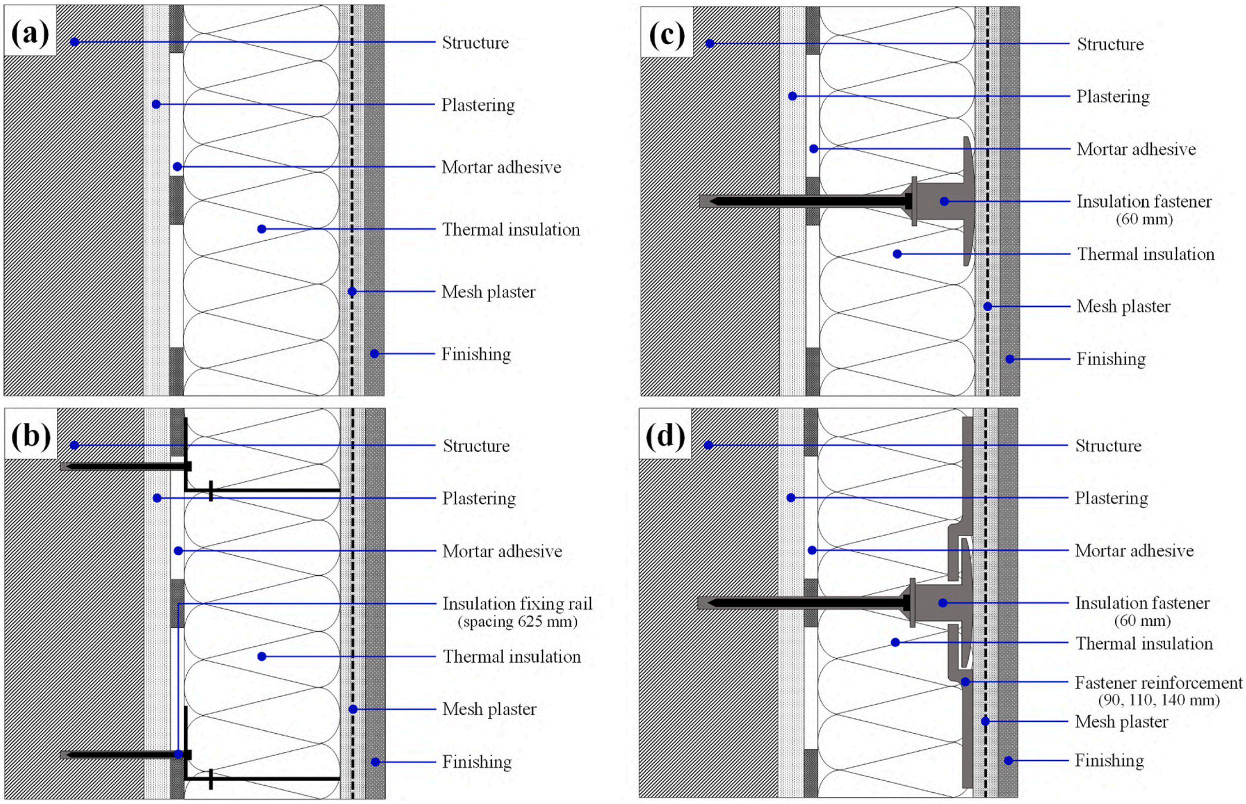

Fig. 1. EIFS construction details: (a) without insulation fastener, (b) with insulation-fixing rail, (c) with insulation fastener, and (d) with insulation fastener (for soft insulation).

thin plaster after installing an insulation material on the exterior of a building. Subsequently, the minimum requirements for exterior wall insulation were established under DIN 4108 in 1969 [18], with the term "exterior insulation finishing system (EIFS)" unified in the 1990s [19].

Fig. 1(a) shows the EIFS construction details without an insulation fastener. The finishing material is used after the insulating material is attached to the plastered structure using a mortar adhesive, while the plastering layer is formed using a mesh. Although a commonly used EIFS method, it is vulnerable to insulation losses or damage [20]. To solve this problem, rails were used to fix the insulation materials in place, as shown in Fig. 1(b). However, in this rail-fixing method, thermal bridges may occur owing to the high thermal conductivity of the metallic rail used in fixing the heat-insulating material [21].

An external insulation method using an insulation fastener has also been used recently to overcome this problem, as shown in Fig. 1 (c). In this approach, plastic nails, which have lower thermal conductivities than metallic nails, are used to fix the insulating materials. These nails can penetrate the structures and fix the insulating materials, thereby preventing the insulating material from detaching or becoming damaged due to external wind pressures. In general, thermal insulation fasteners with a head diameter of 60 mm are used as they feature high fixing forces. Soft insulation materials, such as mineral wool or glass wool, can be fixed more firmly using reinforcing materials, which, in turn, helps improve the fixing force of the fasteners, as shown in Fig. 1(d).

As buildings become taller and more technologically equipped owing to industrial developments and rapid population growth, human and material losses due to fires continue to increase [22,23]. Recently, with the industrial and economic developments in South Korea resulting in steadily increasing urban population density and high-rise and large-scale buildings, building fires have gradually become larger, affecting numerous lives and causing significant property damage. In some recent fire accidents, it was found that the affected buildings had been constructed with materials with poor flame retardancy, which allowed the fire to spread quickly and made it difficult to extinguish, resulting in many casualties because the toxic gas generated during combustion also spread rapidly [24,25]. Based on the fire statistics published by the Korea National Fire Agency [26], building fires account for the highest proportion of fires. Thus, the Ministry of Land, Infrastructure and Transport (MOLIT) amended the "Building Enforcement Decree" on the fire retardant performance of building finishing materials to prevent the spread of fires in buildings [27]. Accordingly, when installing insulation on a building with a height above 9 m (≥3 stories), non-combustible or semi-non-combustible materials must be used or structures that prevent the spread of fire must be constructed, as announced by MOLIT. For buildings with less than five stories (≤22 m high), standards for installing flame retardant materials have also been added. These guidelines also apply to medical, educational research, elderly care, and training facilities. In particular, finishing materials with flame retardant performances exceeding those of semi-non-combustible materials are used for *piloti* buildings that serve as evacuation centers in the event of a fire.

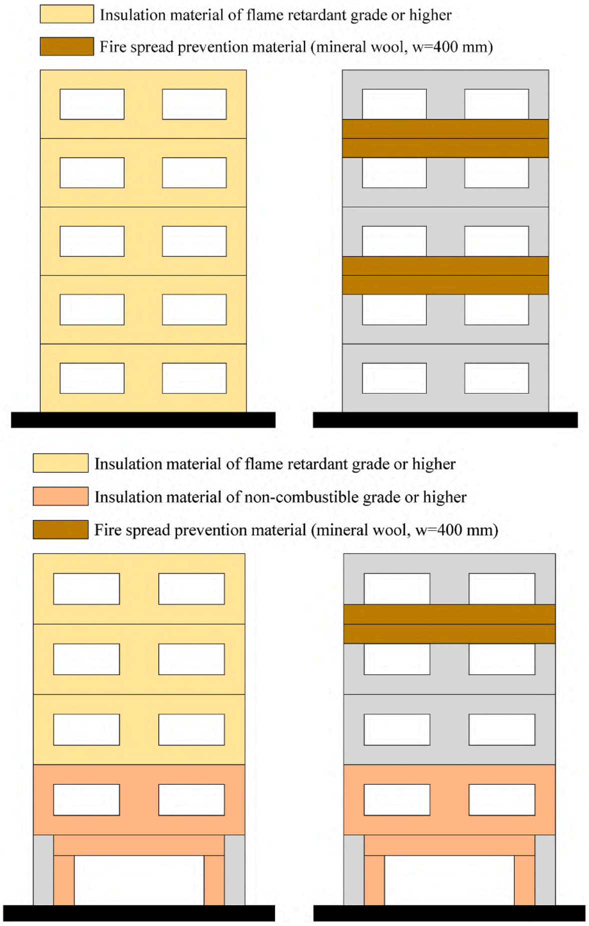

Fig. 2. Schematic of fire spread prevention structure for buildings.

The term "fire spread prevention structure," determined and publicly notified by MOLIT, implies that, in such structures, the space between the material covering the exterior wall and the support structure of this material should be compactly filled with the following materials (at least 400 mm wide on each floor) to prevent vertical fire spread [28]. In particular, in Korea, the following prescriptions exist.

1. Fireproof gypsum boards with sizes of 12.5 mm or larger, as defined by the Korean Industrial Standard KS F 3504 (gypsum board product).
2. Gypsum cement boards of 6 mm or more, as specified in the Korean Industrial Standard KS L 5509 (gypsum cement boards), or flat cement boards of 6 mm or more, as defined in KS L 5114 (fiber-reinforced cement boards).
3. Mineral wool (MW) insulation boards, as specified in the Korean Industrial Standard KS L 9102 (artificial mineral fiber insulation).
4. By the Korean Industrial Standard KS F 2257–8 (fire resistance test method for building members–performance conditions for vertical non-load bearing members), the fire resistance performance test must result in 15 min of flameproof performance, and the material's backside temperature must not rise above 120 K.

Furthermore, for buildings with ≥9 m height (≥3 stories), a fire spread prevention structure needs to be installed every two floors. Fig. 2 shows schematics of the fire spread prevention structure of a five-story building in accordance with the revised law. The amended law stipulates that the entire exterior wall must use an insulating material with a flame-retardant grade or higher or a fire spread prevention material must be used every two floors.

Recently, the global issue of fire spread caused by combustible exterior wall cladding materials has emerged. Consequently, many researchers are studying fires in building exterior walls. Zhang et al. studied melt-flowing and -dripping flames increase fire risks in exterior walls. Bench-scale experiments explored melting-dominant flame spread in EPS foam. Critical fuel coverage and ignition diameter were determined. The study aims to enhance fire protection for building exteriors [29]. Hou et al. investigated upward flame spread in XPS and PU foams under line *n*-heptane fire, noting sustained spread and analyzing burning performance. They revised the relationship between flame height and total heat flux to quantify the fire source's effect on flame-retarded and non-retarded materials [30]. Meng et al. analyzed upward flame spread over XPS foams with varying porosities. Flame height and temperature initially rise, then decrease with increased porosity due to fuel and oxygen competition mechanisms [31]. Recent research on fire in building

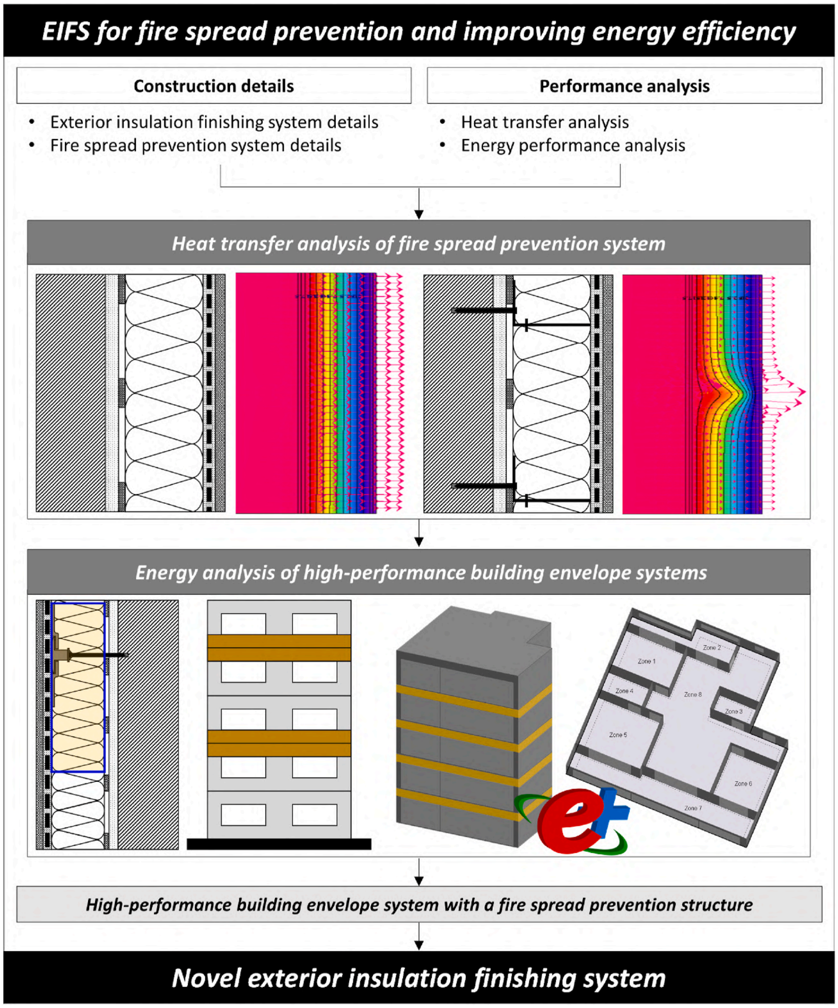

Fig. 3. Research framework.

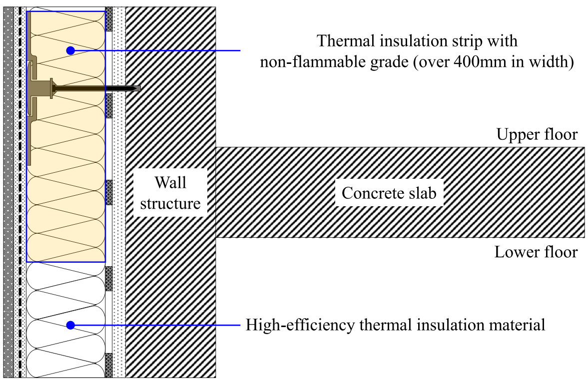

Fig. 4. Details of fire spread prevention structure in EIFS.

exterior walls focuses on flame spread and combustion rates of applied materials. However, this study offers originality and distinctiveness by proposing fire spread prevention structures along with details to enhance thermal performance. Additionally, the phase change materials (PCMs), known to be effective in external wall applications, were employed to achieve a more efficient exterior insulation finishing system. PCMs are substances capable of storing or releasing heat during the phase change process, enabling efficient use of thermal energy. Furthermore, previous research has confirmed that PCM's thermal inertia effect helps maintain indoor

Table 1
Surface heat transfer resistances [35].

Building elements	Heat transfer resistance ($m^2 \cdot K/W$)		
	Indoor surface (R_i)	Outdoor surface (R_o)	
		Direct contact with outdoor air	Indirect contact with outdoor air
The outer wall of living room (Including side walls and windows and doors)	0.11	0.11	0.043
Bottom floor of living room	0.086	0.15	0.043
Ceiling or roof of the living room on the top floor	0.086	0.086	0.043
Intermediate floor of apartment	0.086	–	–

Table 2
Thermal properties of EIFS for ISO 10211 heat transfer analysis.

Materials		Thermal conductivity (W/m·K)	Heat transfer resistance ($m^2 \cdot K/W$)	Volumetric heat capacity ($MJ/m^3 \cdot K$)	Thickness (mm)
Indoor surface			0.04		
Concrete		1.41		1.83	200
Plastering mortar		0.53		1.21	5
Mortar adhesive		0.53		1.21	5
Thermal insulation material	EPS	0.035		0.113	200
	MW	0.037		0.094	
	PF	0.02		0.059	
Fastener	Nail type	0.21		2.259	270
	Rail type	60		3.7	240
Plastering mortar (mesh)		0.53			10
Finishing mortar		0.53			10
Outdoor surface			0.13		

temperatures low and reduces cooling energy consumption [32].

In this study, heat transfer analyses of a building wall with a fire spread prevention structure were performed through HEAT3 simulations to analyze the heat flow. In addition, the annual building energy consumption was calculated using EnergyPlus to derive an energy-efficient building envelope system.

2. Performance analysis

2.1. Analysis framework

Fig. 3 illustrates the flow of analysis in this study. Focusing on two representative details of building exterior wall insulation cladding, thermal transfer analysis is conducted, followed by building energy analysis. Based on this, a building exterior wall finishing system is derived, considering both energy performance improvement with fire spread prevention structures.

2.2. Analyses of heat transfer and energy performance

To reduce the energy consumption of a building and the damage caused by fires, it is necessary to satisfy the standards for the use of high-performance insulation and fire spreading prevention materials. Fire-resistant thermal insulation systems mainly serve to reduce building energy consumption and prevent the spread of fires when they occur. Thus, it is necessary to determine the optimal specifications of non-flammable-grade and high-efficiency thermal insulation materials and evaluate the thermal bridges and energy performance of buildings. Fig. 4 presents the details of a fire spread prevention structure in an EIFS. In an EIFS, thermal bridges may occur through insulation fasteners, metal rails, and fixing nails. Even with an EIFS composed of high-efficiency insulation, thermal bridges must be considered to accurately determine energy efficiency.

2.3. Heat transfer analysis method

In an EIFS, the use of rails and fasteners for fixing insulation materials can cause irregular movement in the heat flow through dissimilar materials with different thermal conductivities. Structural thermal bridges are expected when using bonding materials. DIN 4108 stipulates that these thermal bridges should be analyzed using a technically sufficient and validated method or an accurate thermal bridge verification method. In cases with no thermal bridging standards or without internal insulation applied to the outer shell of a building, an additional value for thermal bridging is recommended to be included. Such thermal bridges can be divided into linear and point thermal bridges, depending on their shapes; linear thermal bridges can occur in balconies, in roof parapets, and around windows. The coefficient of a linear thermal bridge indicates the amount of heat lost or acquired through the linear thermal bridge under the steady state. The ISO 10211 and ISO 14683 standards have been adopted as methods for calculating heat loss through

Table 3
Heat transfer analysis.

EIFS_EPS	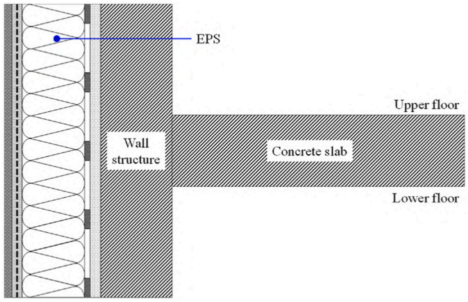
EIFS_EPS_rail	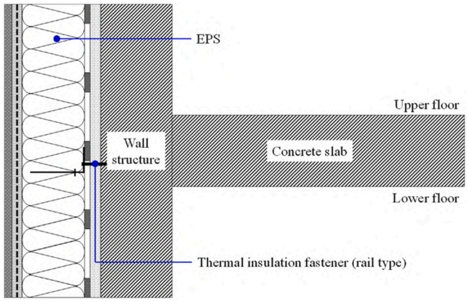
EIFS_EPS_nail	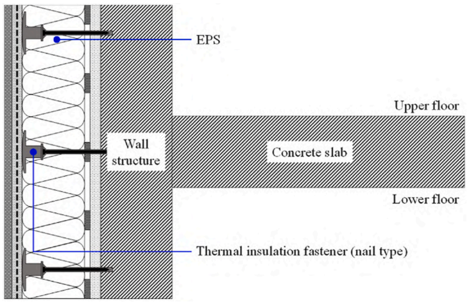
EIFS_MW_EPS_nail	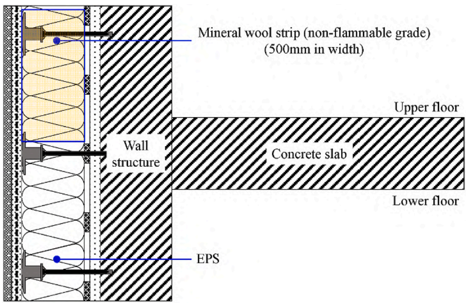

(*continued on next page*)

Table 3 (*continued*)

EIFS_MW_PF_nail	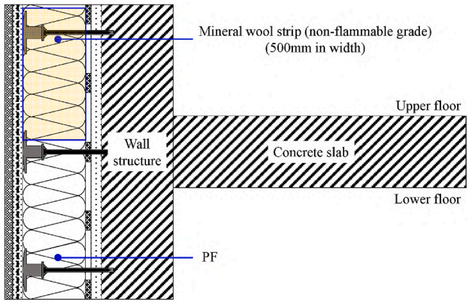
EIFS_PF_nail	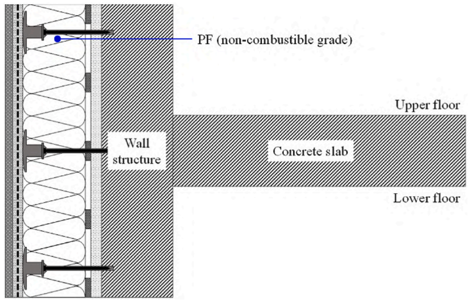

Table 4
Input conditions for simulations of modeled building.

Environmental control	Heating: 20 °C, Relative humidity (R.H.) 50 % Cooling: 26 °C, R.H.* 50 %	
Occupancy schedule	00:00–08:00, 18:00–24:00	100 %
	08:00–18:00	30 %
Metabolic (activity)	130 W/person (Factor: 0.9)	
Lighting density	4.0 W/m^2	
Office equipment	3.0 W/m^2	
Occupancy density	0.05 $person/m^2$	
Infiltration	0.7 ACH	
Ventilation	10 L/s·person	
HVAC	Ideal Loads Air System, Heated floor	
Weather	Seoul, Korea	

Table 5
Construction details of base model.

Construction details		Thickness (mm)	Thermal conductivity (W/m·K)	Density (kg/m^3)	Specific heat capacity (J/kg·K)
External wall (EPS)	Cement plaster	20	0.720	1760	840
	EPS	200	0.040	15	1400
	Cement plaster	20	0.720	1760	840
	Concrete	200	1.400	2100	840
External wall (PF)	Cement plaster	20	0.720	1760	840
	PF board	200	0.020	40	1400
	Cement plaster	20	0.720	1760	840
	Concrete	200	1.400	2100	840
External wall (MW)	Cement plaster	20	0.720	1760	840
	MW	200	0.038	140	840
	Cement plaster	20	0.720	1760	840
	Concrete	200	1.400	2100	840
Floor	Urea-formaldehyde foam	175	0.040	10	1400
	Concrete	100	1.400	2100	840
	EPS	80	0.040	15	1300
	Mortar	30	1.130	2000	1000
Internal wall	Cement plaster	20	0.720	1760	840
	Concrete	100	0.120	530	1600
	Cement plaster	20	0.720	1760	840
Ceiling	Gypsum board	25	0.250	900	1000

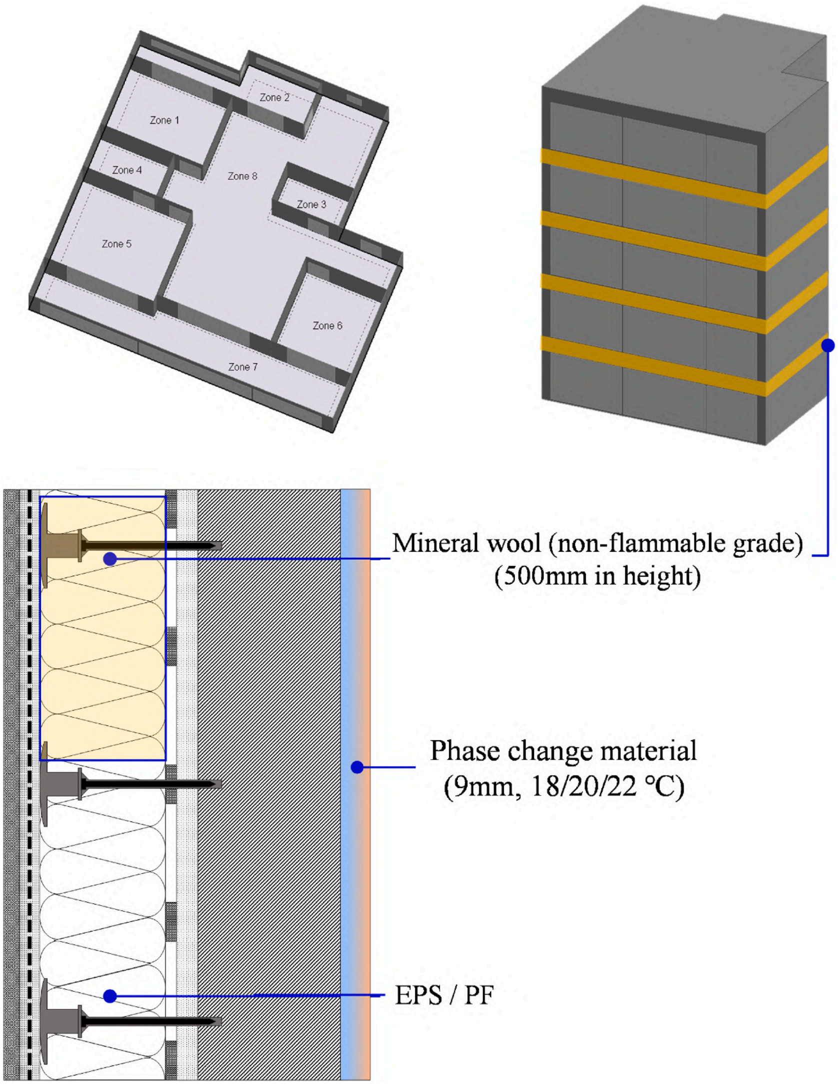

Fig. 5. Perspective view and details of external wall for high-performance building envelope systems.

Table 6
Analysis of high-performance envelope systems with PCM.

Case	Configuration
EPS	Thermal insulation with EPS
EPS_18	EPS +9 mm PCM layer with 18 °C phase change temperature
EPS_20	EPS +9 mm PCM layer with 20 °C phase change temperature
EPS_22	EPS +9 mm PCM layer with 22 °C phase change temperature
MW_EPS	Thermal insulation with EPS and MW (500 mm in height)
MW_EPS_18	MW_EPS + 9 mm PCM layer with 18 °C phase change temperature
MW_EPS_20	MW_EPS + 9 mm PCM layer with 20 °C phase change temperature
MW_EPS_22	MW_EPS + 9 mm PCM layer with 22 °C phase change temperature
MW_PF	Thermal insulation with PF and MW (500 mm in height)
MW_PF_18	MW_PF + 9 mm PCM layer with 18 °C phase change temperature
MW_PF_20	MW_PF + 9 mm PCM layer with 20 °C phase change temperature
MW_PF_22	MW_PF + 9 mm PCM layer with 22 °C phase change temperature
PF	Thermal insulation with PF
PF_18	PF + 9 mm PCM layer with 18 °C phase change temperature
PF_20	PF + 9 mm PCM layer with 20 °C phase change temperature
PF_22	PF + 9 mm PCM layer with 22 °C phase change temperature

Table 7
Heat transfer analysis results (EIFS_EPS).

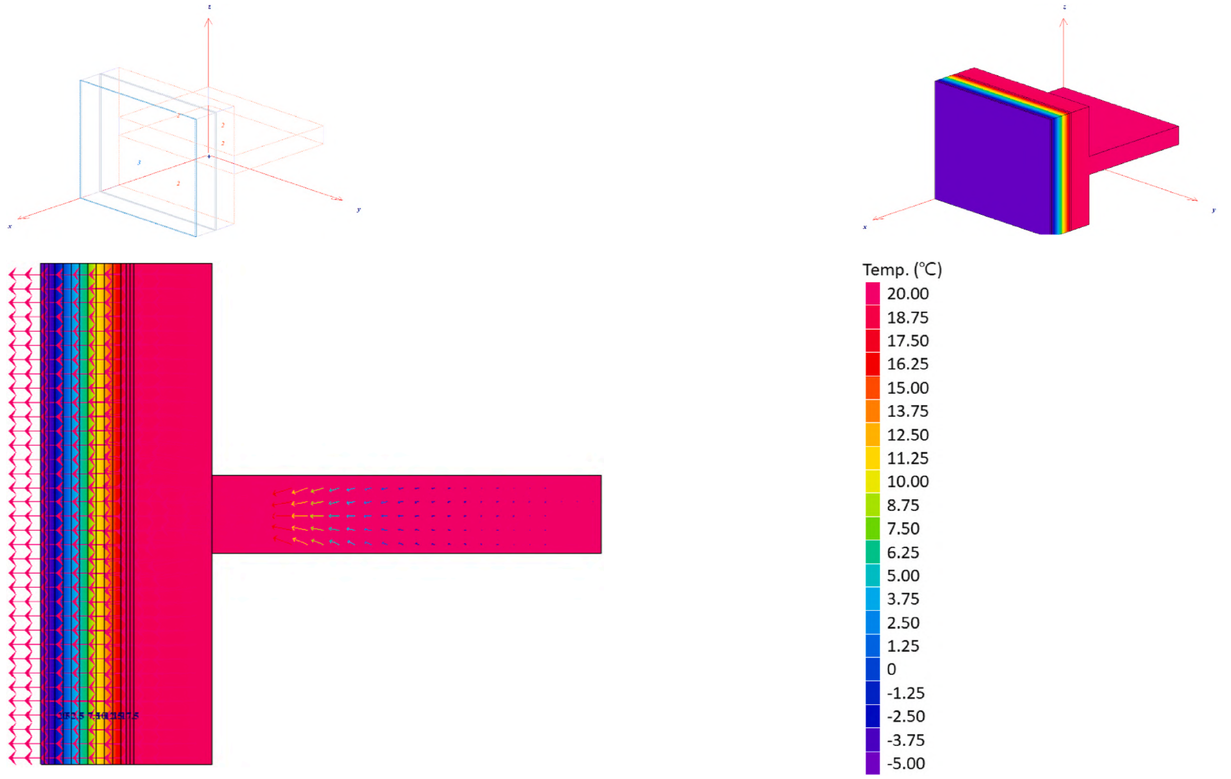

Thermal coupling matrix L3D: 0.2575 W/K
Heat flow using L3D: 6.4368 W

thermal bridges [33,34]. Moreover, ISO 14683 serves as a method for estimating heat loss through approximations, by standardizing the main areas where thermal bridges occur.

The thermal performance was analyzed using BLOCON HEAT3 for an EIFS using both fire-resistant structures and high-efficiency thermal insulation materials. According to the calculation method of ISO 10211, which specifies the thermal bridge surface temperature and heat flow of a building, the exact amount of heat transfer can be determined, including that from the thermal bridge transmitted through the wall. The equivalent and linear thermal transmittance rates were calculated using the following equations:

$$U_{eq} = \frac{Q}{\Delta T \bullet A}, \tag{1}$$

$$U_{eq} = U_i + \frac{\sum_j l_j \psi_j}{A}, \tag{2}$$

$$\psi = \frac{Q}{\Delta T} - (U_i \bullet l_i), \tag{3}$$

where U_{eq} is the equivalent thermal transmittance (W/m^2·K), ΔT is the temperature difference between the inside and outside (°C), A is the surface area (m^2), Q is the total heat flow of the wall (W), U_i is the thermal transmittance of material i (W/m^2·K), l_i is the length of the thermal transmittance of U_i (m), and ψ is the linear thermal transmittance (W/m·K).

The outdoor temperature was set to −5 °C, and the indoor temperature was set to 20 °C, according to DIN 4108–2. In addition, for an accurate heat transfer analysis, the surface heat transfer resistances generated from the indoor and outdoor surfaces were considered. Therefore, as listed in Table 1, a thermal transfer analysis was performed considering the indoor and outdoor surface heat transfer resistances, as specified in the current building code.

ISO 10211 stipulates that, when calculating and modeling the amount of heat flow through a structure, the symmetry line should serve as the standard in the case of a continuous section; however, its length should be modeled to be at least three times the wall thickness or 1000 mm, whichever is greater. Therefore, the length of the case considered in this study was set as 1290 mm. The thermal properties of the EIFS for the ISO 10211 heat transfer analysis are listed in Table 2. The simulations analyzed four cases of EIFS walls

Table 8
Heat transfer analysis results (EIFS_EPS_rail).

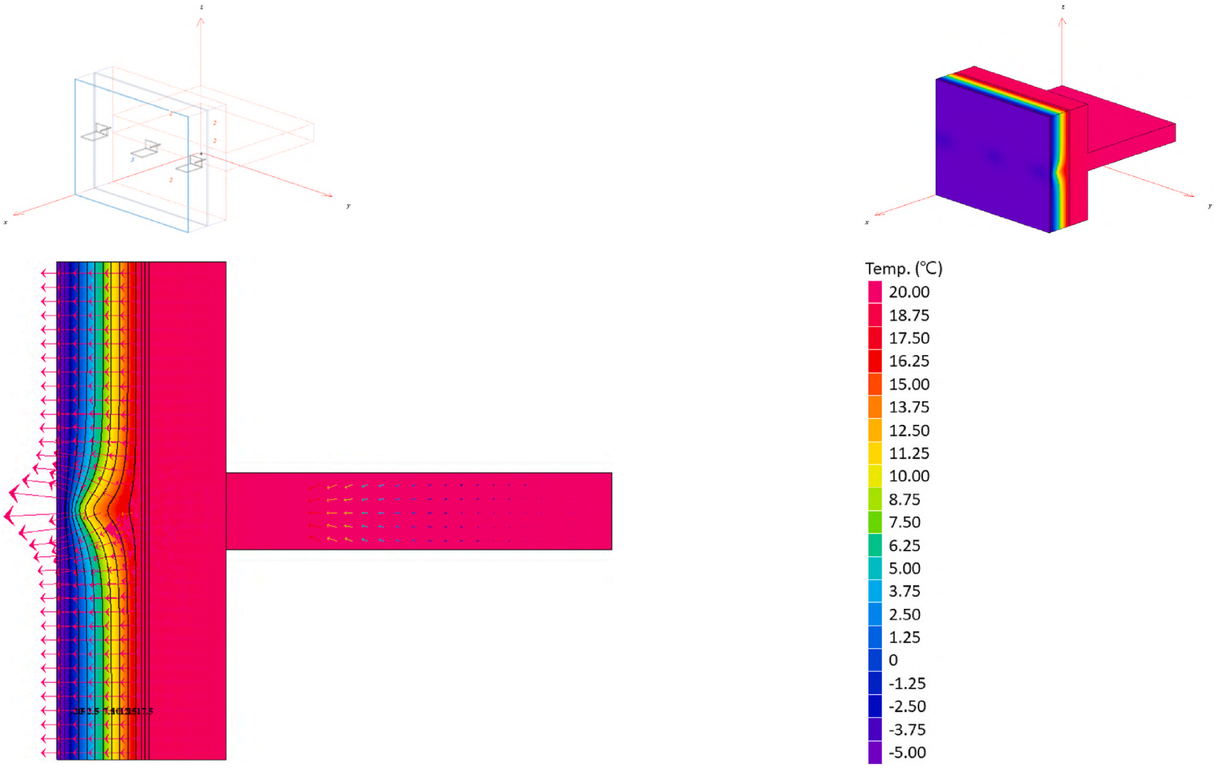

Thermal coupling matrix L3D: 0.2839 W/K
Heat flow using L3D: 7.0977 W

using expanded polystyrene (EPS), MW, and/or phenolic foam (PF) as insulation material—EPS_nail (EPS), MW_EPS_nail (MW_EPS), MW_PF_nail (MW_PF), and PF_nail (PF)—as presented in Table 3.

2.4. Energy performance analysis

DesignBuilder version 5.4 was used to evaluate the energy performance of the fire and thermal insulation systems of the buildings. DesignBuilder uses the EnergyPlus tool, which was developed by the US Department of Energy, to dynamically simulate the energy consumption of a building.

In this analysis, the model was based on a typical Korean apartment, as shown in Table 4. A typical Korean apartment was selected from the open architectural database provided by the Ministry of Land, Infrastructure, and Transport (MOLIT) of South Korea [36]. The input conditions for each building component of the model are presented in Table 5. This model was simulated by constructing an exterior wall using combustible EPS, semi-non-combustible-grade PF, and non-combustible-grade MW as the variables.

2.5. High-performance building envelope systems

Fig. 5 shows a high-efficiency building insulation system using a phase change material (PCM). The PCM improves the thermal storage performance of buildings, enabling the efficient use of heat, thus resulting in reduced building energy consumption. The PCM applied to the inside of the model featured a thickness of 9 mm, thermal conductivity of 0.2 W/m·K, specific heat of 1970 J/kg·K, and density of 235 kg/m^3. Phase change temperatures of 18, 20, and 22 °C were selected to maintain an appropriate indoor temperature during winter, considering the climate characteristics of South Korea, where the heating energy is higher than the cooling energy [37, 38]. Table 6 presents the analysis of the high-efficiency insulation system in which the PCM was applied.

3. Results and discussion

3.1. Heat transfer analysis results

Table 7 shows the results of the heat transfer analysis for the EIFS_EPS case, constructed without an insulation fastener; notably, it exhibited excellent thermal results because there were no broken areas in the insulation; in addition, thermal bridges did not occur. Furthermore, the thermal coupling matrix L3D value for the EIFS_EPS case was 0.257 W/K, and the heat flow using L3D was 6.4368 W. Table 8 shows the EIFS_EPS_rail case, where the rail-type fastener was composed of steel and exhibited a thermal conductivity of 60 W/

Table 9
Heat transfer analysis results (EIFS_EPS_nail).

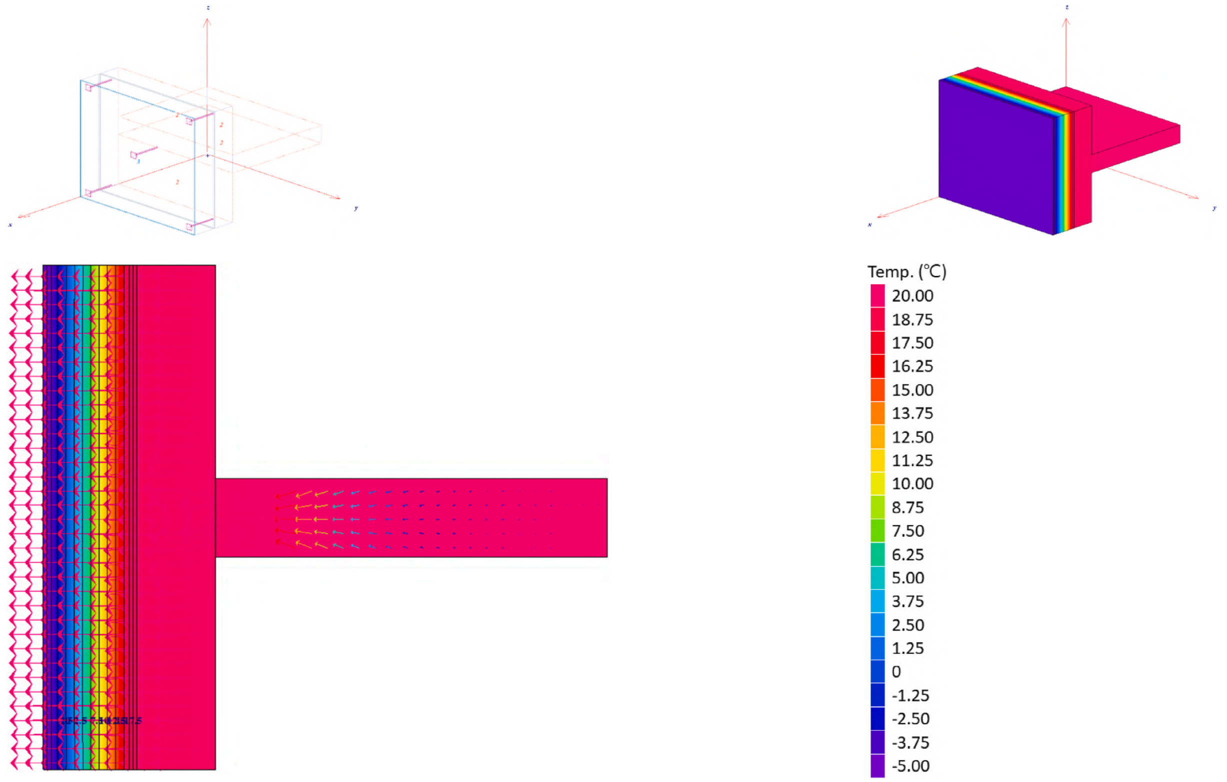

Thermal coupling matrix L3D: 0.2581 W/K
Heat flow using L3D: 6.4516 W

m·K. Therefore, the heat transfer through the steel rail was high, and heat loss occurred in the areas where the insulator was fixed with this rail. In addition, the thermal coupling matrix L3D value was 0.2839 W/K, and the heat flow using L3D was 7.0977 W. Thus, it was confirmed that the heat loss was 10.3 % higher than that in the EIFS_EPS case. Table 9 shows the results of the heat transfer analysis for the EIFS_EPS_nail case. As a plastic nail with a thermal conductivity of 0.21 W/m·K (which is significantly lower than that of steel) was used, the thermal bridging caused by the fasteners was negligible. The thermal coupling matrix L3D value of the EIFS_EPS case was 0.2581 W/K, and the heat flow using L3D was 6.4516 W. Thus, the heat flow increased by 0.2 %, as compared with that in the EIFS_EPS case, where no insulation fastener was used. Therefore, using nail-type insulation fasteners was deemed excellent for fixing insulation materials. Table 10 lists the results of the heat transfer analysis for the EIFS_MW_EPS_nail case, where the insulation applied to the fire spread prevention structure was non-flammable-grade MW at a thickness of 500 mm, and the thermal conductivity was 0.038 W/m·K. Owing to the difference in the thermal conductivities when using EPS, the thermal coupling matrix L3D was 0.2701 W/K, and the heat flow using L3D was 6.7529 W; compared with the EIFS_EPS_nail case, the heat flow was somewhat increased. This was attributed to the increase in the thermal transmittance of the fire spread prevention structure. Table 11 presents the results of the heat transfer analysis for the EIFS_MW_PF_nail case, where MW was used as the material for the fire spread prevention structure and PF was used for the other insulation materials. The thermal conductivity of the PF was 0.020 W/m·K. The thermal coupling matrix L3D value was 0.2109 W/K, and the heat flow using L3D was 5.2734 W. Compared with that for the EIFS_EPS_nail case, the heat flow was reduced by 18.1 %. This was attributed to the low thermal conductivity of PF. Table 12 shows the results of the heat transfer analysis for the EIFS_PF_nail case, where the entire external wall was applied with PF, which is a non-combustible insulation material. The requirements of the fire spread prevention structure were satisfied, even when the entire external wall was non-combustible. The thermal coupling matrix L3D was 0.1611 W/K, and the heat flow using L3D was 4.0284 W. This indicated a 37.4 % decrease in the heat flow, as compared with the EIFS_EPS case.

The results of the heat transfer analyses for each case are shown in Table 13. The two types of fasteners used to secure the insulation material to the exterior wall, as presented in Table 2, have thermal conductivity values of 0.21 W/m·K for the nail type and 60 W/m·K for the rail type. Due to this difference in thermal conductivity, the rail-type fastener was found to exhibit rapid heat flow along this area, leading to a pronounced thermal bridging effect. In contrast, the nail-type fastener showed a stable heat flow similar to that of the insulation material, attributed to its lower thermal conductivity. In addition, when there was a difference in the thermal conductivity of the insulation material and the fire spread prevention structure, the heat flow was concentrated toward the material with higher

Table 10
Heat transfer analysis results (EIFS_MW_EPS_nail).

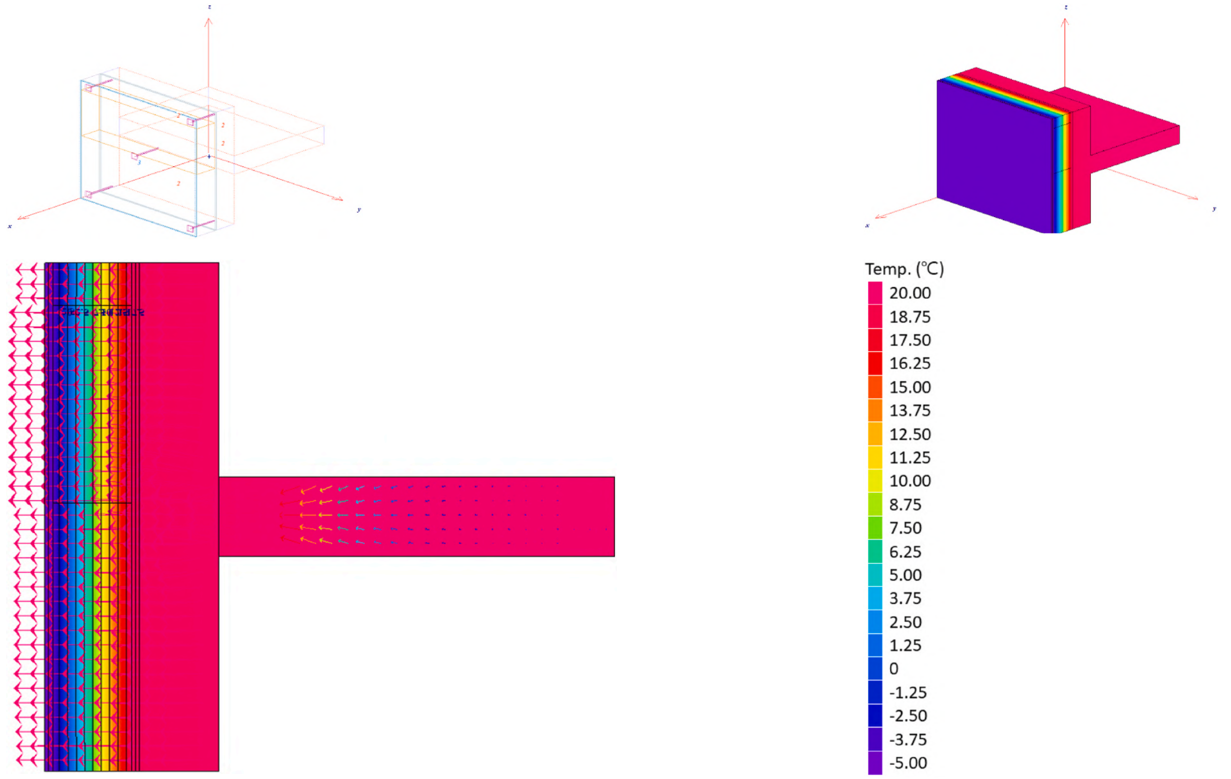

Thermal coupling matrix L3D: 0.2701 W/K
Heat flow using L3D: 6.7529 W

thermal conductivity. The total amount of heat transfer differed by up to 37.4 %, depending on the thermal conductivity of the insulation applied to the exterior wall.

3.2. Results of energy performance analysis

In prior research, to validate the reliability of building energy performance, actual indoor temperature measurements were compared and analyzed alongside temperature change data obtained through simulation predictive analysis. In previous studies, the coefficient of variation of the root mean square error (CV(RMSE)) was utilized for comparison and verification [39]. Fig. 6 shows the results of the analyses of the heating, cooling and annual energy consumption under the four cases, respectively. It was found that the heating energy consumption for the EIFS building was lower than that the internal insulation system of the building because the efficiency of thermal energy use was higher [17]. For MW_EPS, the heating energy consumption tended to increase because a 500-mm-thick layer of MW, which features a higher thermal conductivity than EPS, was applied to the fire spread prevention structure between each floor. However, for MW_PF, the overall heating energy decreased because the thermal conductivity of PF was 0.02 W/m·K.

Contrary to the results for the heating energy consumption, the cooling energy consumption tended to increase with the insulation performance. In general, heat loss was reduced in the buildings using high-efficiency thermal insulation materials. This is because the heat generated indoors, such as that from the human body, lighting, and machines, cannot be dissipated. It was found that the heating energy consumption during winter was low because of the use of high-efficiency thermal energy in the EIFS buildings; however, the cooling energy consumption was high because the cooling load in summer increases owing to the decrease in heat loss. Fig. 7 shows the results of the analyses of the total annual energy consumption for the four cases. The EPS case involved an EIFS building with no fire spread prevention structure, whereas the MW_EPS, MW_PF, and PF cases entailed EIFS buildings with fire spread prevention structures. Compared with the EPS case, the overall energy consumption in the MW_EPS case increased. However, the energy consumption in MW_PF and PF was reduced by 8.8 % and 9.9 %, respectively. As shown in Table 2, the thermal conductivity of EPS was 0.035 W/m·K, while that of PF was 0.02 W/m·K. The use of insulation materials with low thermal conductivity resulted in reduced energy consumption due to lower heat energy loss. Thus, a fire-resistant thermal insulation system can reduce energy consumption, while satisfying the requirement of the fire spread prevention structure.

Table 11
Heat transfer analysis results (EIFS_MW_PF_nail).

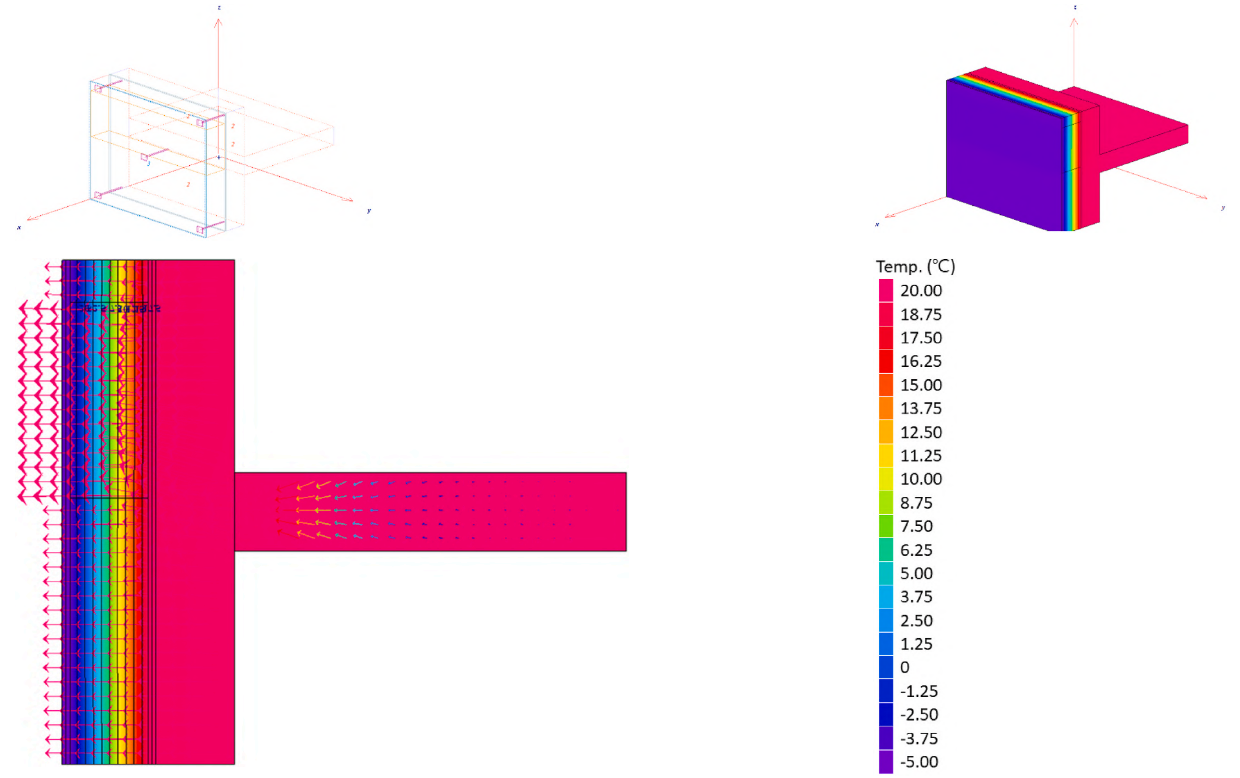

Thermal coupling matrix L3D: 0.2109 W/K
Heat flow using L3D: 5.2734 W

3.3. *Results of energy performance analysis for high-performance building envelope systems*

Fig. 8 shows the building energy simulation results. In buildings with a PCM, an average reduction of 3 % in building energy consumption was noted, as compared with that before PCM application. In addition, when the PCM was applied to the inner side of the exterior insulation system of a building with the fire spread prevention structure, an additional reduction of 2 % was achieved in the building energy consumption. The largest building energy reduction was observed when a PCM with a phase change temperature of 20 °C was applied. This was because the PCM had the highest heat storage performance; the indoor temperature in winter was between 18 °C and 22 °C. Compared with EPS, where the PCM was absent, the building energy consumption in PF, with the PCM featuring a phase change temperature of 20 °C, decreased by 11.9 %. In terms of simply reducing the annual energy consumption, the building envelope system with PF alone was concluded to be the best. However, when considering fire safety, the building envelope systems with both MW and PF afforded excellent results in terms of both thermal and fire safety performance.

4. Conclusions

EIFSs efficiently utilize building thermal energy but face issues with mortar adhesive weaknesses leading to detachment and fire spread risks. Fastener-based solutions exist, yet metal rails create thermal bridges. This study proposes an EIFS method fixing insulation from outside, enhancing thermal efficiency. Heat transfer analysis informs this method's development. Energy simulations focus on fire spread prevention, highlighting the importance of EIFS with high thermal efficiency. Heat transfer analysis revealed that using metal rails increased heat flow by 10.3 %, while plastic nails maintained similar heat flow to mortar adhesives. Applying non-combustible PF to the entire exterior wall reduced heat flow by 37.4 %, meeting fire spread prevention requirements. A building energy demand assessment showed a slight increase in total consumption with MW between floors compared to EPS alone. However, energy consumption decreased by 8.8 % with MW and PF, and by 9.9 % with PF alone on the exterior wall. Using PCM in an external insulation system reduced energy consumption by up to 11.9 %, emphasizing the importance of energy reduction and fire safety. Among the cases established in this study, the configuration involving a fire spread prevention zone using mineral wool, followed by external insulation with PF and PCM (MW_PF_20), was evaluated as the optimal case, successfully achieving both fire safety performance and energy efficiency. This study systematically proposes measures to enhance both the fire prevention structure of building exteriors in accordance with Korean regulations and energy efficiency improvement. However, it is limited by the scope of analysis constrained by Korean regulations. In future research, will be focusing to numerically apply fire safety-related systems from

Table 12
Heat transfer analysis results (EIFS_PF_nail).

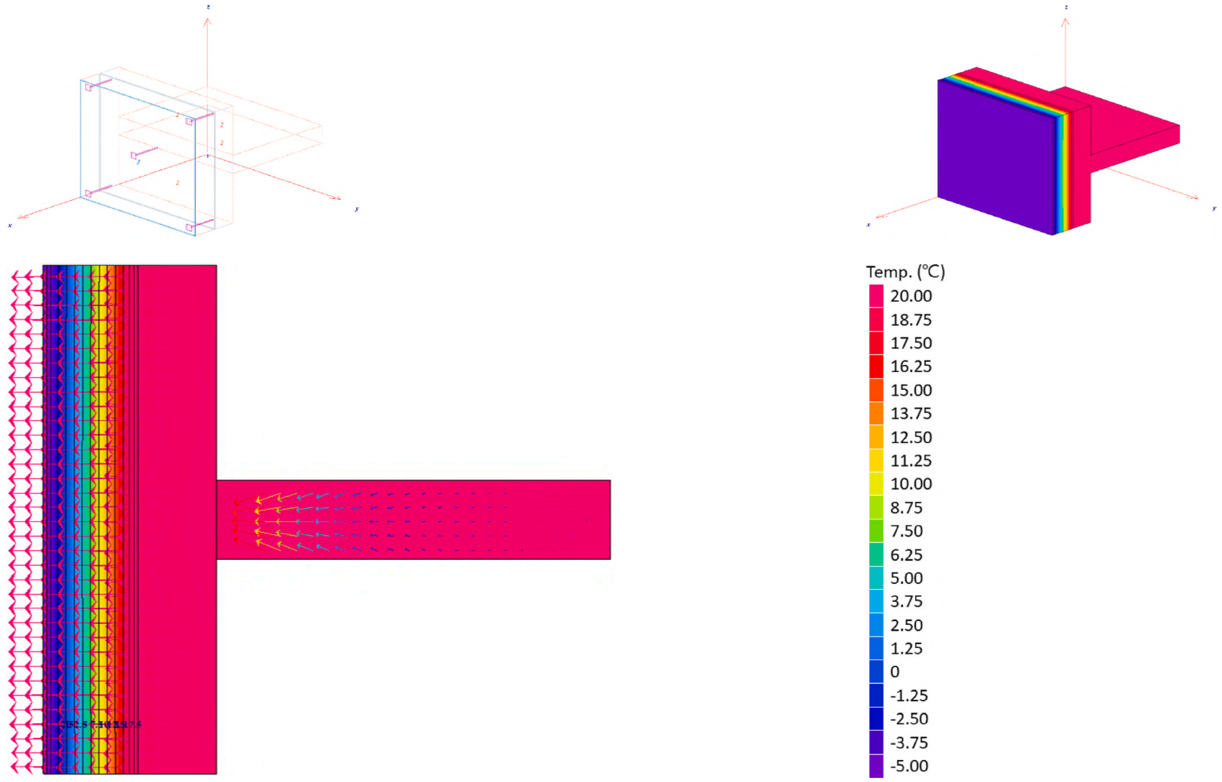

Thermal coupling matrix L3D: 0.1611 W/K
Heat flow using L3D: 4.0284 W

Table 13
Heat flow for each case.

Case	Thermal coupling matrix L3D (W/K)	Heat flow using L3D (W)	Difference in rate with EIFS_EPS (%)
EIFS_EPS	0.257	6.4368	–
EIFS_EPS_rail	0.283	7.0977	10.3
EIFS_EPS_nail	0.258	6.4516	0.2
EIFS_MW_EPS_nail	0.270	6.7529	4.9
EIFS_MW_PF_nail	0.210	5.2734	−18.1
EIFS_PF_nail	0.161	4.0284	−37.4

representative countries such as the United States, Europe, and Asia and analyze trends specific to each country.

Fire spreadfire spreadfire spread.

CRediT authorship contribution statement

Seunghwan Wi: Writing – original draft, Conceptualization. **Young Uk Kim:** Resources. **Seong Jin Chang:** Visualization. **Umberto Berardi:** Formal analysis. **Sumin Kim:** Supervision.

Declaration of competing interest

The authors declare that they have no known competing financial interests or personal relationships that could have appeared to influence the work reported in this paper.

Data availability

Data will be made available on request.

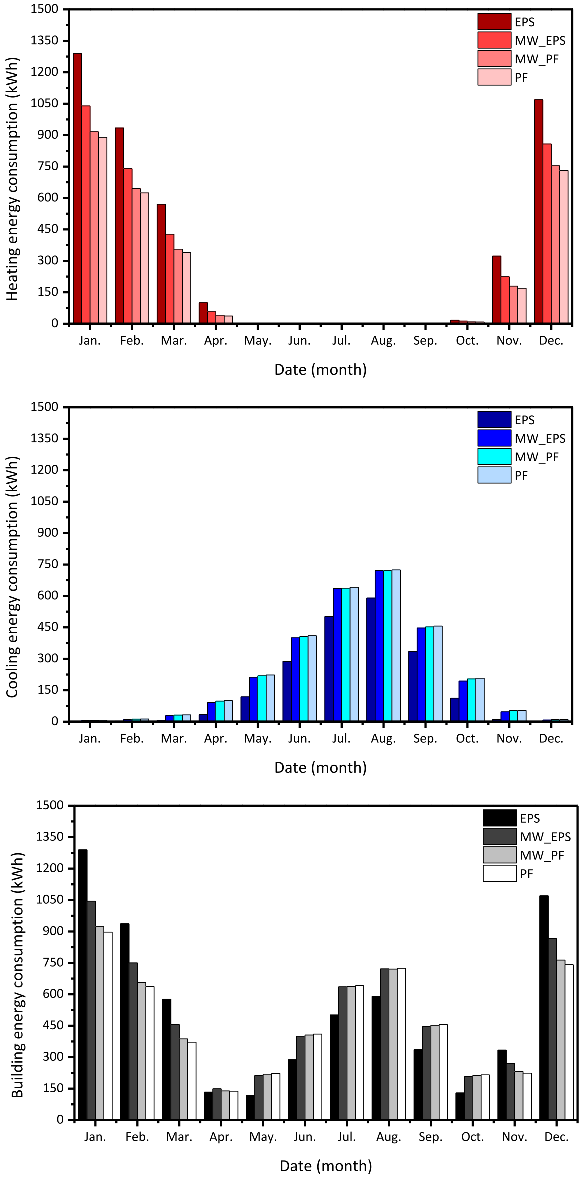

Fig. 6. Results of energy consumption.

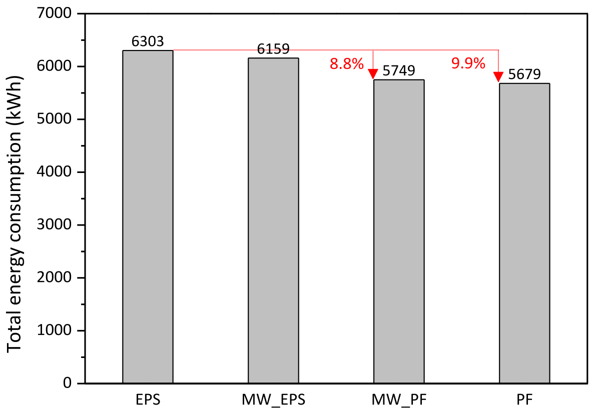

Fig. 7. Results of total annual energy consumption.

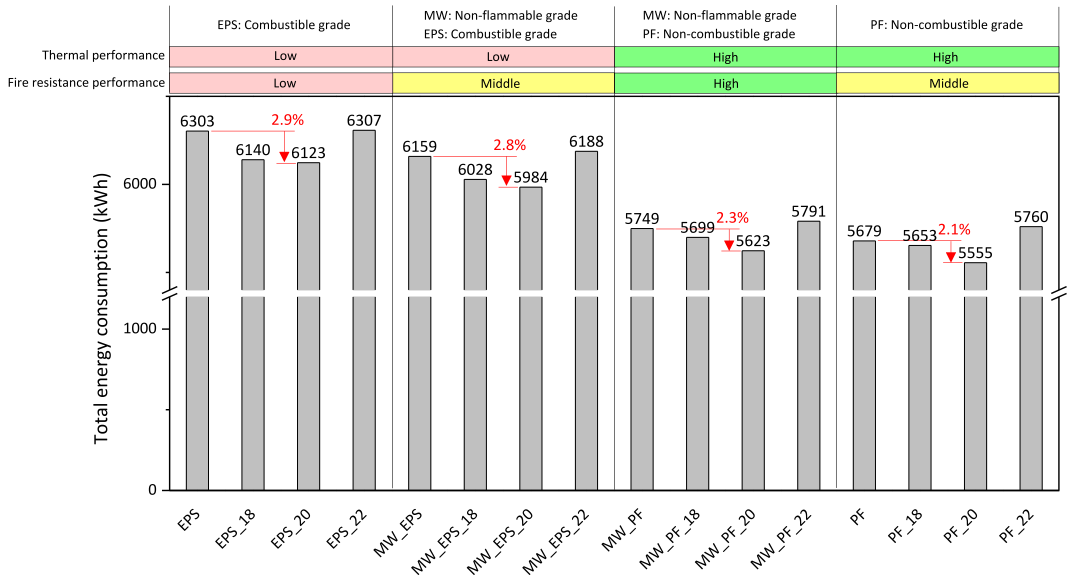

Fig. 8. Analysis results for high-performance building envelope systems.

Acknowledgements

This work was supported by the National Research Foundation of Korea (NRF) grant funded by the Korea government (MSIT) (No. 2022R1C1C2010049).

References

[1] A. Kasaeian, L. bahrami, F. Pourfayaz, E. Khodabandeh, W.-M. Yan, Experimental studies on the applications of PCMs and nano-PCMs in buildings: a critical review, Energy Build. 154 (2017) 96–112, https://doi.org/10.1016/J.ENBUILD.2017.08.037.
[2] Q. Wang, R. Wu, Y. Wu, C.Y. Zhao, Parametric analysis of using PCM walls for heating loads reduction, Energy Build. 172 (2018) 328–336, https://doi.org/10.1016/J.ENBUILD.2018.05.012.
[3] I. Ari, R. Sari, Differentiation of developed and developing countries for the Paris Agreement, Energy Strategy Rev. 18 (2017) 175–182, https://doi.org/10.1016/J.ESR.2017.09.016.
[4] I. Deák Lakatos, U. Berardi, Thermal characterization of different graphite polystyrene, Int. Rev. Appl. Sci. Eng. 9 (2018) 163–168, https://doi.org/10.1556/1848.2018.9.2.12.
[5] S. Wi, U. Berardi, S. Di Loreto, S. Kim, Microstructure and thermal characterization of aerogel–graphite polyurethane spray-foam composite for high efficiency thermal energy utilization, J. Hazard Mater. 397 (2020) 122656, https://doi.org/10.1016/j.jhazmat.2020.122656.
[6] W. Yang, J. Liu, Y. Wang, S. Gao, Experimental study on the thermal conductivity of aerogel-enhanced insulating materials under various hygrothermal environments, Energy Build. 206 (2020) 109583, https://doi.org/10.1016/j.enbuild.2019.109583.
[7] Á. Lakatos, Stability investigations of the thermal insulating performance of aerogel blanket, Energy Build. 185 (2019) 103–111, https://doi.org/10.1016/j.enbuild.2018.12.029.
[8] Y.U. Kim, S.J. Chang, Y.-J. Lee, H. No, G.S. Choi, S. Kim, Evaluation of the applicability of high insulation fire door with vacuum insulation panels: experimental results from fire resistance, airtightness, and condensation tests, J. Build. Eng. 43 (2021) 102800.

[9] S. Fantucci, S. Garbaccio, A. Lorenzati, M. Perino, Thermo-economic analysis of building energy retrofits using VIP - vacuum Insulation Panels, Energy Build. 196 (2019) 269–279, https://doi.org/10.1016/j.enbuild.2019.05.019.
[10] S. Fantucci, A. Lorenzati, A. Capozzoli, M. Perino, Analysis of the temperature dependence of the thermal conductivity in Vacuum Insulation Panels, Energy Build. 183 (2019) 64–74, https://doi.org/10.1016/j.enbuild.2018.10.002.
[11] S. Wi, S. Yang, U. Berardi, S. Kim, Assessment of recycled ceramic-based inorganic insulation for improving energy efficiency and flame retardancy of buildings, Environ. Int. 130 (2019), https://doi.org/10.1016/j.envint.2019.06.010.
[12] B. Chal, B. Yrieix, L. Roiban, K. Masenelli-Varlot, J.-M. Chenal, G. Foray, Nanostructured silica used in super-insulation materials (SIM), hygrothermal ageing followed by sorption characterizations, Energy Build. 183 (2019) 626–638, https://doi.org/10.1016/j.enbuild.2018.11.044.
[13] U. Berardi, C. Sprengard, An overview of and introduction to current researches on super insulating materials for high-performance buildings, Energy Build. 214 (2020) 109890, https://doi.org/10.1016/j.enbuild.2020.109890.
[14] U. Berardi, L. Ákos, Thermal bridges of metal fasteners for aerogel-enhanced blankets, Energy Build. 185 (2019) 307–315, https://doi.org/10.1016/J.ENBUILD.2018.12.041.
[15] D. Borelli, P. Cavalletti, A. Marchitto, C. Schenone, A comprehensive study devoted to determine linear thermal bridges transmittance in existing buildings, Energy Build. 224 (2020) 110136, https://doi.org/10.1016/j.enbuild.2020.110136.
[16] T.G. Theodosiou, A.G. Tsikaloudaki, K.J. Kontoleon, D.K. Bikas, Thermal bridging analysis on cladding systems for building facades, Energy Build. 109 (2015) 377–384.
[17] T. Kisilewicz, M. Fedorczak-Cisak, T. Barkanyi, Active thermal insulation as an element limiting heat loss through external walls, Energy Build. 205 (2019) 109541, https://doi.org/10.1016/j.enbuild.2019.109541.
[18] THERMAL PROTECTION AND ENERGY ECONOMY IN BUILDINGS - PART 2: MINIMUM REQUIREMENTS TO THERMAL INSULATION, DIN 4108, 1969.
[19] T. Information, P. Series, Exterior Insulation and Finishing Systems, 1997.
[20] S. Kim, J. Seo, H. Jeong, J. Kim, In situ measurement of the heat loss coefficient of thermal bridges in a building envelope, Energy Build. 256 (2022) 111627.
[21] T. Theodosiou, K. Tsikaloudaki, S. Tsoka, P. Chastas, Thermal bridging problems on advanced cladding systems and smart building facades, J. Clean. Prod. 214 (2019) 62–69.
[22] N. Wang, Y. Gao, C. ying Li, W. mei Gai, Integrated agent-based simulation and evacuation risk-assessment model for underground building fire: a case study, J. Build. Eng. 40 (2021) 102609, https://doi.org/10.1016/J.JOBE.2021.102609.
[23] P. Yang, X. Tan, H. Sun, D. Chen, C. Li, Fire accident reconstruction based on les field model by using orthogonal experimental design method, Adv. Eng. Software 42 (2011) 954–962, https://doi.org/10.1016/J.ADVENGSOFT.2011.05.041.
[24] J.P. Hidalgo, S. Welch, J.L. Torero, Performance criteria for the fire safe use of thermal insulation in buildings, Construct. Build. Mater. 100 (2015) 285–297, https://doi.org/10.1016/J.CONBUILDMAT.2015.10.014.
[25] M. Konecki, J. Gałaj, Flame transfer through the external walls insulation of the building during a fire, Procedia Eng. 172 (2017) 529–535, https://doi.org/10.1016/J.PROENG.2017.02.062.
[26] Korea National Fire Agency, Statistical Yearbook of National Fire Agency, 2019.
[27] Regulations on standards for evacuation and fire protection of buildings, Ministry of Land Infrastructure and Transport, 2019.
[28] Flame retardant performance test of building finishing materials, Ministry of Land Infrastructure and Transport, n.d.
[29] M. Zhang, Y. Wang, M. Li, F. Gou, J. Sun, Experimental investigation of downward discrete flame spread of the thermoplastic material in exterior insulation walls: melt-flowing and -dripping, Fire Saf. J. 136 (2023) 103754, https://doi.org/10.1016/J.FIRESAF.2023.103754.
[30] Y. Hou, X. Cheng, S. Liu, C. Liu, H. Zhang, Experimental study on upward flame spread of exterior wall thermal insulation materials, Energy Proc. 66 (2015) 161–164, https://doi.org/10.1016/J.EGYPRO.2015.02.085.
[31] Q.X. Meng, G.Q. Zhu, M.M. Yu, Z.H. Liang, Experimental study on upward flame spread characteristics of external thermal insulation material under the influence of porosity, Case Stud. Therm. Eng. 12 (2018) 365–373, https://doi.org/10.1016/J.CSITE.2018.05.008.
[32] S. Wi, S.J. Chang, S. Kim, Improvement of thermal inertia effect in buildings using shape stabilized PCM wallboard based on the enthalpy-temperature function, Sustain. Cities Soc. 56 (2020) 102067, https://doi.org/10.1016/J.SCS.2020.102067.
[33] I.S.O. En, Thermal Bridges in Building Construction-Heat Flows and Surface Temperatures-Detailed Calculations, 2017.
[34] I.O. for Standardization, Thermal Bridges in Building Construction: Linear Thermal Transmittance: Simplified Methods and Default Values, ISO, 2007.
[35] Building Energy Saving Design Standards, Ministry of Land, Infrastructure and Transport, Republic of Korea, n.d.
[36] Ministry of Land, Infrastructure, and Transport (MOLIT), Architectural Data Open System, 2019.
[37] D.G. Atinafu, B.Y. Yun, S. Yang, H. Yuk, S. Wi, S. Kim, Structurally advanced hybrid support composite phase change materials: architectural synergy, Energy Storage Mater. 42 (2021) 164–184, https://doi.org/10.1016/J.ENSM.2021.07.022.
[38] J.H. Park, J. Jeon, J. Lee, S. Wi, B.Y. Yun, S. Kim, Comparative analysis of the PCM application according to the building type as retrofit system, Build. Environ. 151 (2019) 291–302, https://doi.org/10.1016/J.BUILDENV.2019.01.048.
[39] J.H. Park, U. Berardi, S.J. Chang, S. Wi, Y. Kang, S. Kim, Energy retrofit of PCM-applied apartment buildings considering building orientation and height, Energy 222 (2021) 119877, https://doi.org/10.1016/J.ENERGY.2021.119877.